Guidelines for Deployment of Area-Array Packages in Harsh Environments

N. Singh, P. Lall
Center for Advanced Vehicular Electronics (CAVE)
Department of Mechanical Engineering
Auburn University
Auburn, AL 36849
(334) 844-3424 (phone)
lall@eng.auburn.edu (E-mail)

OBJECTIVE
Development of guidelines for selection and deployment of area-array packages in harsh environments.

Who is the End-User of the Guidelines
Government Contractors, OEMs, and 3rd party contract manufacturers who intend to select part architectures and board designs based on specified mission requirements.

What the guidelines do NOT specify?
Guidelines document does not specify the required level of component reliability for use in various mission critical applications.

Architectures, geometry or materials for use in specific environments are not specified.

The guidelines are not a comprehensive library of every component that can be used in harsh environments.

Scope of the Guidelines
Aid for understanding the sensitivity of component reliability to geometry, package architecture, material properties and board attributes to enable educated selection of appropriate components.

The guidelines have been developed as tool for doing trade-offs between geometry, materials and quantitatively evaluating the impact on reliability.

Guidelines Modules
Establishment of overall mission requirements for which the package is to be designed

Package reliability database for different area array packages

Sensitivity of geometry, architecture and material parameters based on statistical analysis.

Development of sensitivity relations for geometry, materials, and architectures based on physics-of-failure based closed form models.

Inputs

The inputs to the use of design guidelines include - mission requirements, geometry or space constraints within which and IC package or part needs to reside, reliability required for application environment, mechanical functional requirements including number of I/O, Pitch, ball size, die ratio. In this version of the guidelines document, only thermal environments will be considered.

- Environment
  Thermal- max & min temperatures, cycling frequency and gradients
  Mechanical- vibration levels
  Moisture or humidity level

- Geometry or space constraints

- Reliability
  Thermal cycle life requirements
  Vibration life requirement

- Electrical- Number of I/O

Guidelines for package selection:

For package selection the NASA space missions can be divided into four broad categories [Ghaffarian 1998, 2003]

A- Mild thermal cycle exposure with short missions duration
B- Mild thermal cycle exposure with long missions duration
C- Extreme thermal cycles with short mission duration
D- Extreme thermal cycles with long mission duration

- Most PBGAs on polymeric circuit boards can meet the requirements of A and B missions.
- PBGAs with large die may not be used or may be qualified for use under B category.

- Low I/O ceramic packages(<400I/O) may be sufficient for A but should be verified for B missions.
- High I/O ceramic packages(>500I/O) may not be used for either A or B categories.
- Most ceramic and plastic CSPs may meet A mission requirements but may be required to be qualified for B,C, and D mission categories.

Parameters to be considered for design of an area array packages:
There are several factors or considerations which affect the reliability of the area array packages:

-Component size
-Die size
-Die to package ratio
-Solder ball composition (lead-free versus eutectic, 63Sn/37Pb, 62Sn/36Pb/2Ag, 60Sn/40Pb)
-Solder joint size (joint area and height)
-Solder stencil thickness & solder volume
-Ball pitch and ball count
-Array configuration (Perimeter or full array)
-Underfill
-Conformal coat
-Pad size
-Pad configuration (SMD/NSMD)
-Solder mask thickness and opening diameter
-CTE mismatch between mold compound, under-fill material and BT laminate
-Global CTE mismatch between component and PWB board
-PWB thickness
-Surface finish (HASL, OSP, Au)
-PWB laminate material
-Via-in-pad effects on reliability

Die to package ratio:

The reliability of a ball-grid array package generally decreases with the increase in the die-to-package ratio. Packages with smaller die should be preferred for missions with excessive thermal cycling exposure. This effect has been demonstrated in both rigid-substrate and flex-substrate packages. Packages with compliant elastomeric substrates (e.g. μBGA) do not exhibit this effect. This ratio is often referred to as the packaging ratio in literature.

Thermal reliability test [Darveaux et al. 2000] was conducted to study the effect of die/body ratio on the solder joint thermal fatigue life of different sizes of BGA packages. Thermal cycle of –40°C to 125°C with 15mins ramps and 15mins dwells was used for the test. 8mm, 12mm, 15mm, 16mm, 17mm and 27mm FlexBGA packages with different die sizes were used in the test. The cycles for 1% failure from the experimental data and the statistical model has been plotted against the die to body ratio of the various packages. Four layer FR-4 test boards of 0.85mm and 1.6mm thickness with OSP finish and SMD pads were used for the air to air thermal cycling test.

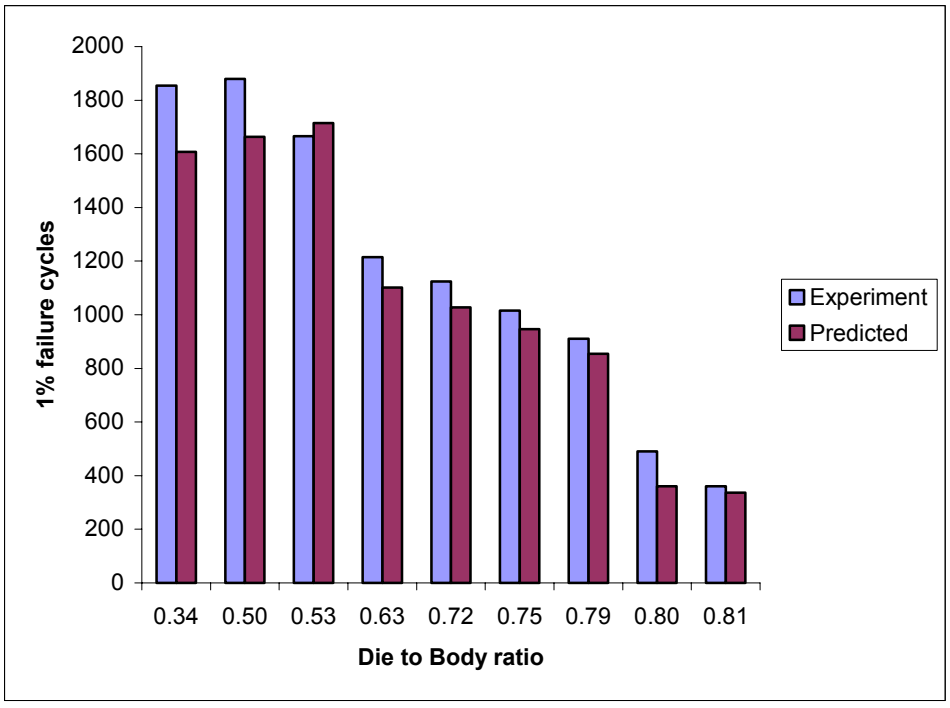

Figure 1: Effect of die-to-package ratio on thermal fatigue reliability of BGA subjected to –40 to 125 °C Thermal Cycle.

The predicted curve from the statistical model follows the experimental curve quite accurately and shows the same trend. The general trend is decrease in thermal reliability of the package with increase in the die to body ratio of the

package, except for the one package with die to body ratio of 0.65. This is due to the fewer number(96) of solder balls in this package as compared to the other packages(132-381). The table below shows the exact comparison of experimental failure data with that of predicted failure life from the statistical model for BGAs with different die-to-body ratio.

Die-to-Body Ratio	Ball Count	Ball Dia (mm)	Experim-ental	Multivariate Regression Model $t_{ref} - S_k\Delta$	Sensitivity Factor for Die-to-Body Ratio, S_k
0.34	40	0.45	1855	1607	-1.17
0.50	280	0.45	1880	1663	
0.53	280	0.45	1666	1715	
0.63	208	0.45	1215	1101	
0.65	96	0.30	780	723	
0.72	280	0.45	1124	1027	
0.75	132	0.45	1016	946	
0.79	144	0.45	911	855	
0.80	208	0.45	491	360	
0.81	96	0.30	360	337	

Ball Count:

The experimental thermal reliability data [Darveaux et al. 2000] indicates that the reliability of the BGAs increases with the increase in the ball count of the package. The cycles for 1% failure from the experimental data and the statistical model have been together plotted against the ball count for different BGA sizes. The experimental data used for the purpose includes 7.5mm, 8mm, 12mm, 15mm and 16mm FlexBGA packages.

The Fig.2 indicates a close agreement between the experimental data and the statistical model predictions. The general trend of increase in thermal reliability with the increase in the ball count can be seen from the plot, which is in agreement with the physics of failure. With the increase in the number of solder balls the thermal load acting on the solder joints gets distributed and the stress level in the individual ball decreases. The packages with ball count of 40 and 144 show a reverse trend, but this is due to the coupling of other effects which overshadow the effect of ball count on the thermal reliability. The BGA with ball count of 40 has unexpectedly high life which can be attributed to a very low die-to-body ratio of 0.34 for this package as compared to body ratio of 0.53 to 0.81 of other packages. The BGA with 144 balls also shows reverse trend, which is due to high mold compound filler content in this particular package.

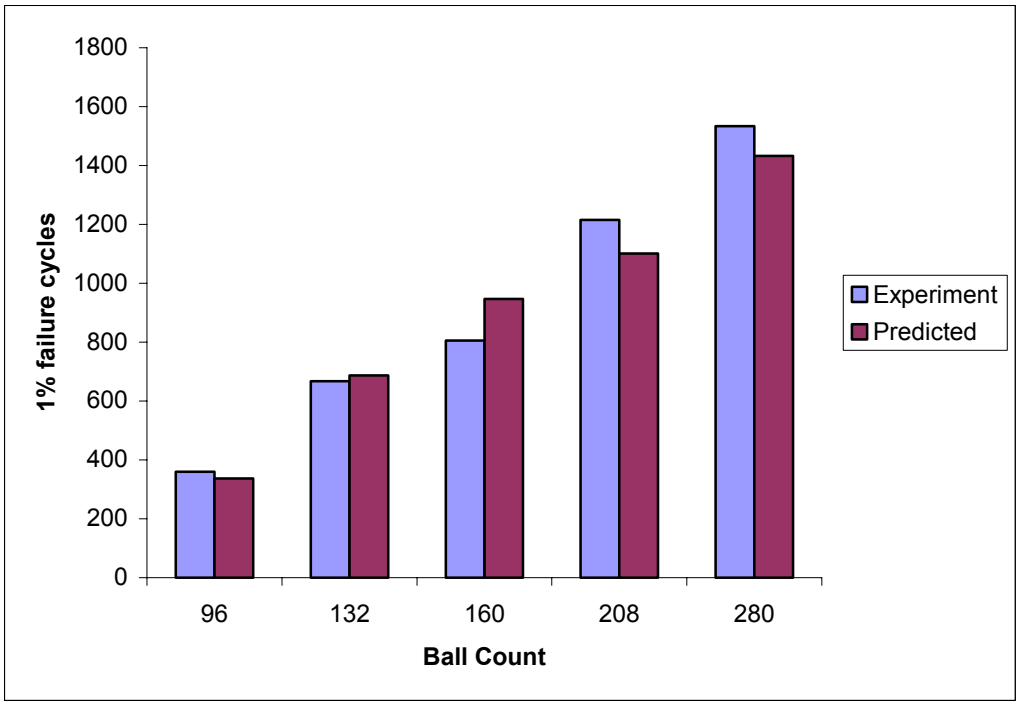

Figure 2: Effect of ball count on thermal fatigue reliability of BGA subjected to –40 to 125 °C Thermal Cycle.

Ball Count	Die-to-Body Ratio	Mold Compound Filler Content	Experi-mental	Multivariate Regression Model $t_{ref} - S_k\Delta$	Sensitivity Factor for Ball Count, S_k
40	0.34	1	1855	1607	0.00105
96	0.81	1	360	337	
132	0.79	1	667	687	
144	0.79	0	475	548	
160	0.49	1	805	947	
208	0.63	1	1215	1101	
280	0.72	1	1534	1433	

Ball Diameter:

The ball diameter has a pronounced effect on the thermal reliability of the BGA packages. The increase in the ball diameter leads to overall better thermal reliability of the package. The experimental thermal reliability data [Darveaux et al. 2000] compared with the statistical model predictions consisted of the BGA packages with solder ball diameter of 0.30mm, 0.45mm and 0.50mm. The plot in the Fig.3 depicts the accurate prediction of 1% failure cycles for BGA with variable ball diameter. Clear trend of increase in thermal fatigue life of the package with increase in the ball diameter is evident from the figure. This trend is in compliance with the theory of failure mechanics as the increase in the solder ball diameter increases the crack area resulting in higher thermal fatigue life.

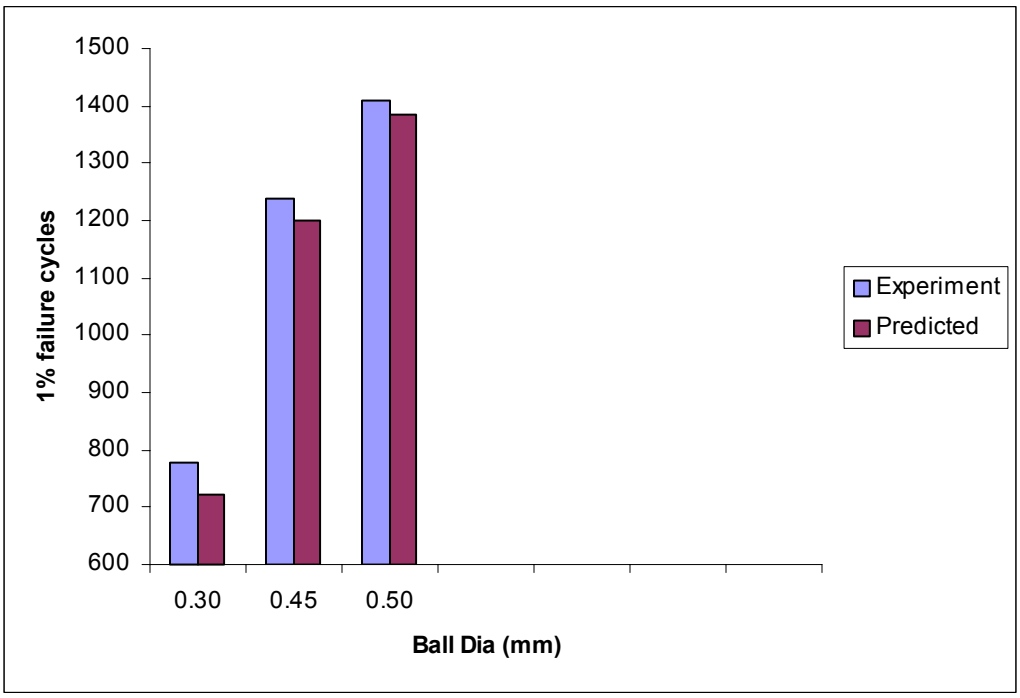

Figure 3: Effect of solder ball diameter on thermal fatigue reliability of BGA subjected to –40 to 125 °C Thermal Cycle.

Ball Diameter (mm)	Experimental	Multivariate Regression Model $t_{ref} - S_k\Delta$	Sensitivity Factor for Ball Diameter, S_k
0.30	778	723	1.24
0.45	1238	1201	
0.50	1408	1386	

Board thickness:

The reliability of a ball-grid array package generally decreases with the increase in the PCB thickness. This effect has been demonstrated in both rigid-substrate and flex-substrate packages. Packages with compliant elastomeric substrates (e.g. μBGA) do not exhibit this effect. Sensitivity factor has been computed from the multivariate regression model for PCB thickness in the range of 0.85 mm to 1.6mm

Darveaux et al. [2000] conducted thermal reliability tests on 0.85mm and 1.6mm thick 4-layer FR-4 boards to investigate the effect of board thickness on the solder joint reliability of different sizes of FlexBGA packages. 8mm, 12mm, 15mm and 16mm FlexBGAs with different die/body ratios were selected for the test. All the packages except for the 16mm FlexBGA with die to body ratio of 0.53 and ball count of 280 show degradation in thermal reliability with the increase in the board thickness. This trend may be attributed to the increase in the assembly stiffness due to increase in the PCB thickness leading to higher stresses in the solder balls due to the CTE mismatch. This opposite trend is due to the high mold compound filler content used for the packages on 0.85mm PCB. So the effect of PCB thickness is reversed due to the high filler content in the mold compound. Thermal cycle of –40°C to 125°C with 15mins ramp and 15mins dwell was used for the test.

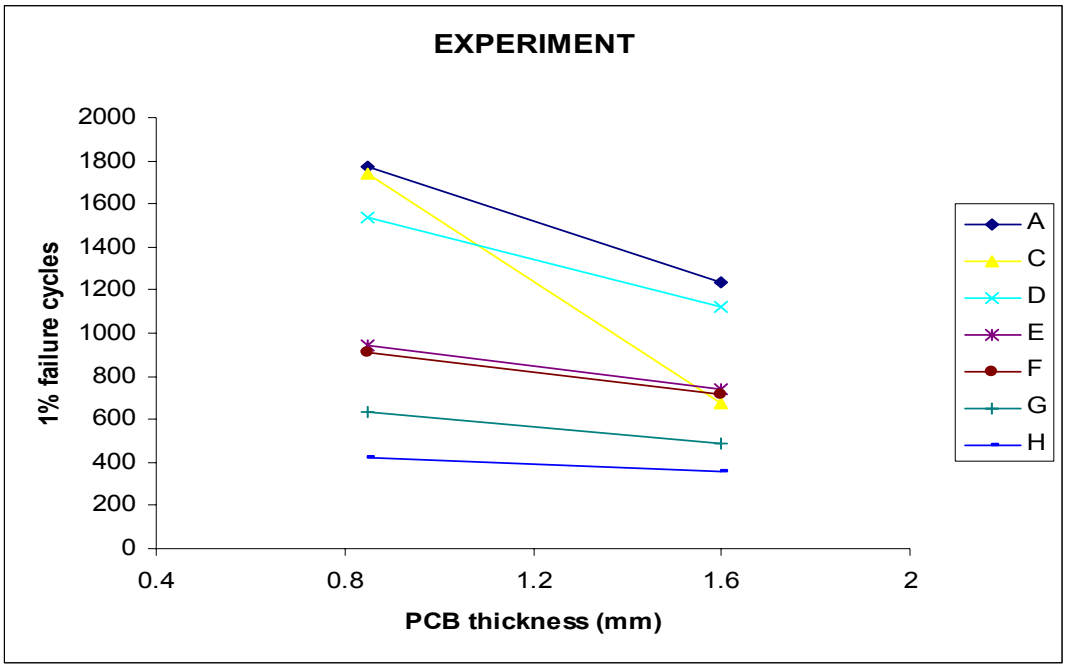

Figure 4 Exp. data plot for FlexBGA with die-to-package ratios between 0.53 and 0.81, subjected to –40 to 125 °C Thermal Cycle and PCB thickness 0.85 and 1.60mm

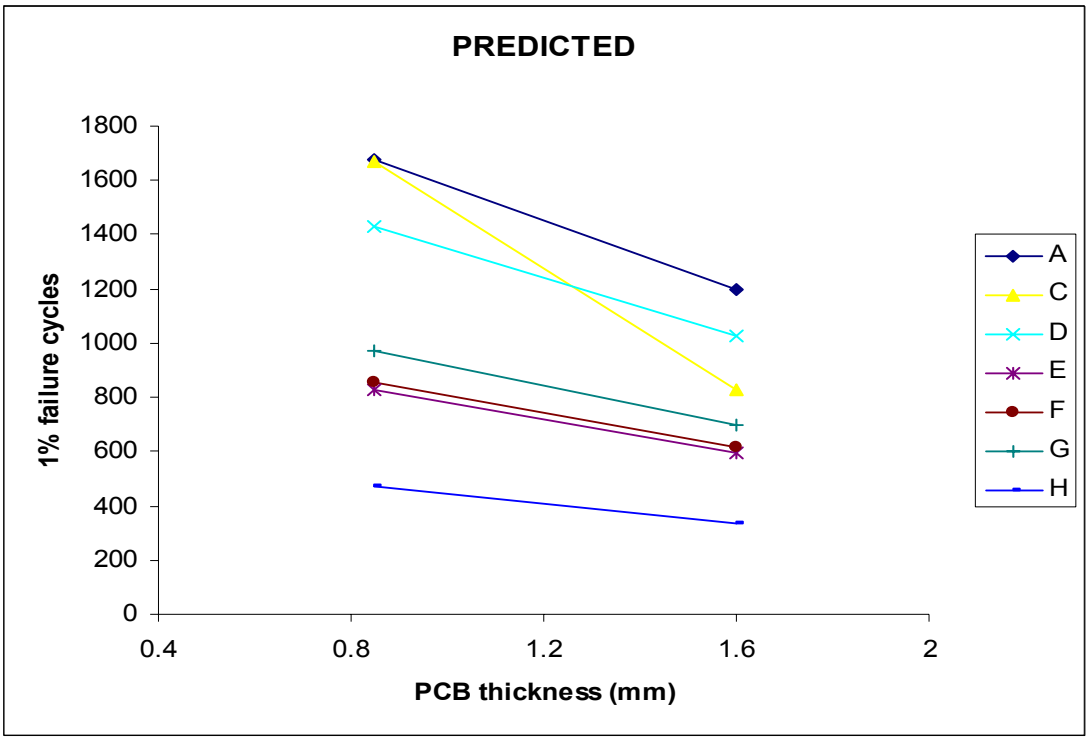

Figure 5 Statistical model prediction plot for FlexBGA with die-to-package ratios between 0.53 and 0.81, subjected to –40 to 125 °C Thermal Cycle and PCB thickness 0.85 and 1.60mm

The experimental X-factor calculated from the two different PCB thicknesses has been compared with that of predicted values based on the statistical model in the table below.

S.No.	Die-to-Body Ratio; Ball Count	Experimental X-Factor	Multivariate Regression Model	Sensitivity Factor for PCB Thickness, S_k
A.	0.53; 132	0.70	0.72	-0.193
B.	0.53; 280	1.29	1.12	
C.	0.54; 132	0.39	0.50	
D.	0.72; 280	0.73	0.72	
E.	0.79; 132	0.79	0.72	
F.	0.79; 144	0.79	0.72	
G.	0.80; 208	0.77	0.72	
H.	0.81; 96	0.86	0.72	

Mold Compound Filler Content:

The thermal reliability of the BGA package decreases with the increase in the mold compound filler content. The BGA with lower amount of the mold compound filler have better thermal fatigue reliability. This trend is visible in the plots for two different 16mmFlexBGA packages with die-to-body ratio of 0.53 and 0.72. The value of 0 indicates high filler content and the value of 1 indicates low filler content. Both the curves have nearly same slope, which implies the correct prediction of the sensitivity of the component's thermal reliability to the mold compound filler content. This trend is consistent from the failure mechanics point of view as the higher filler content mold compound will have higher elastic modulus and a lower CTE. Higher modulus of elasticity make the package stiffer, so more stresses will be transmitted to the solder joints and lower CTE will increase both the local and global thermal expansion mismatch. Both contributing to poor thermal fatigue reliability of the package.

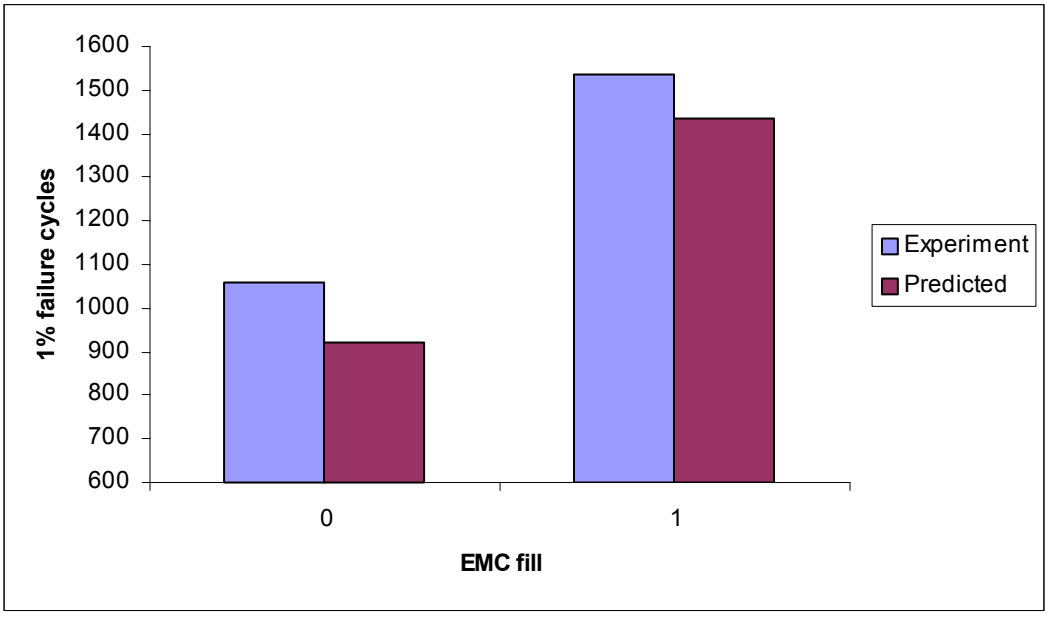

Figure 6 Effect of mold compound filler content on thermal fatigue reliability of 16mm FlexBGA with die-to-body ratio 0.53, subjected to –40 to 125 °C Thermal Cycle

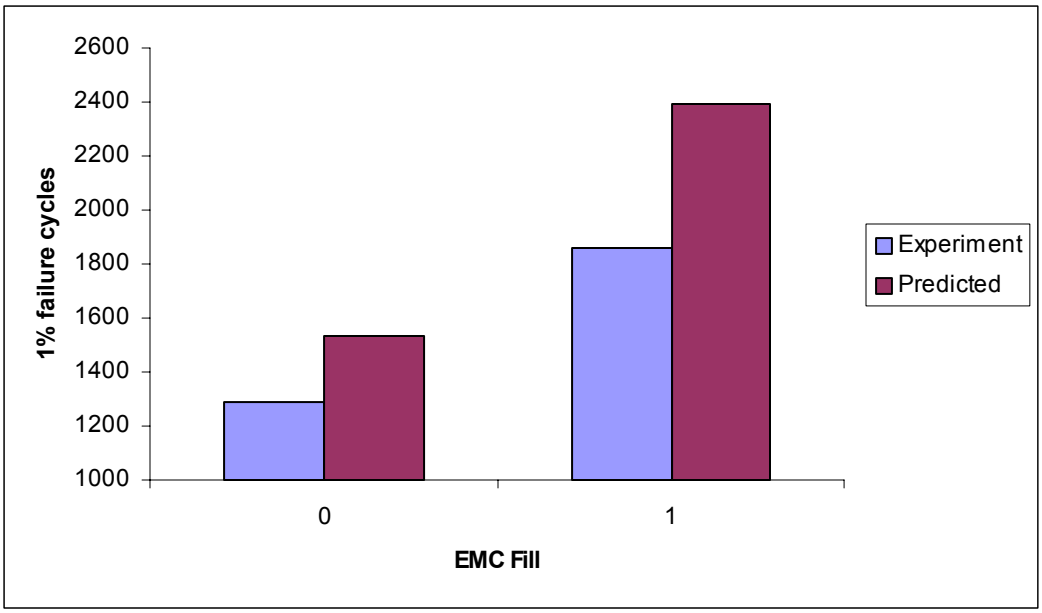

Figure 7 Effect of mold compound filler content on thermal fatigue reliability of 16mm FlexBGA with die-to-body ratio 0.72, subjected to –40 to 125 °C Thermal Cycle

Die-to-Body Ratio (Device)	Experimental X-Factor	Multivariate Regression Model	Sensitivity Factor for EMC fill, S_k
0.53	0.69	0.64	0.193
0.72	0.69	0.64	

Pad Configuration (SMD/NSMD):

Solder joint reliability in thermal fatigue increases with change in mask definition from SMD to NSMD. This trend is visible from the 1% failure plot for 15mm, 160 I/O FlexBGA. The value of 0 indicates SMD pad configuration and the value 1 indicates NSMD pad configuration in the plot. This effect is true for both rigid-substrate and flex-substrate ball grid array packages. Packages with compliant elastomeric substrates (e.g. μBGA) do not exhibit this effect. This trend may vary depending on the mode of failure. The package may show opposite trend in case the failure is due to the tearing out of the laminate under bending as shown by Mawer et. al.[1996]. In that case the solder mask of the SMD pad helps to anchor the pad to the laminate core which leads to better thermal fatigue reliability.

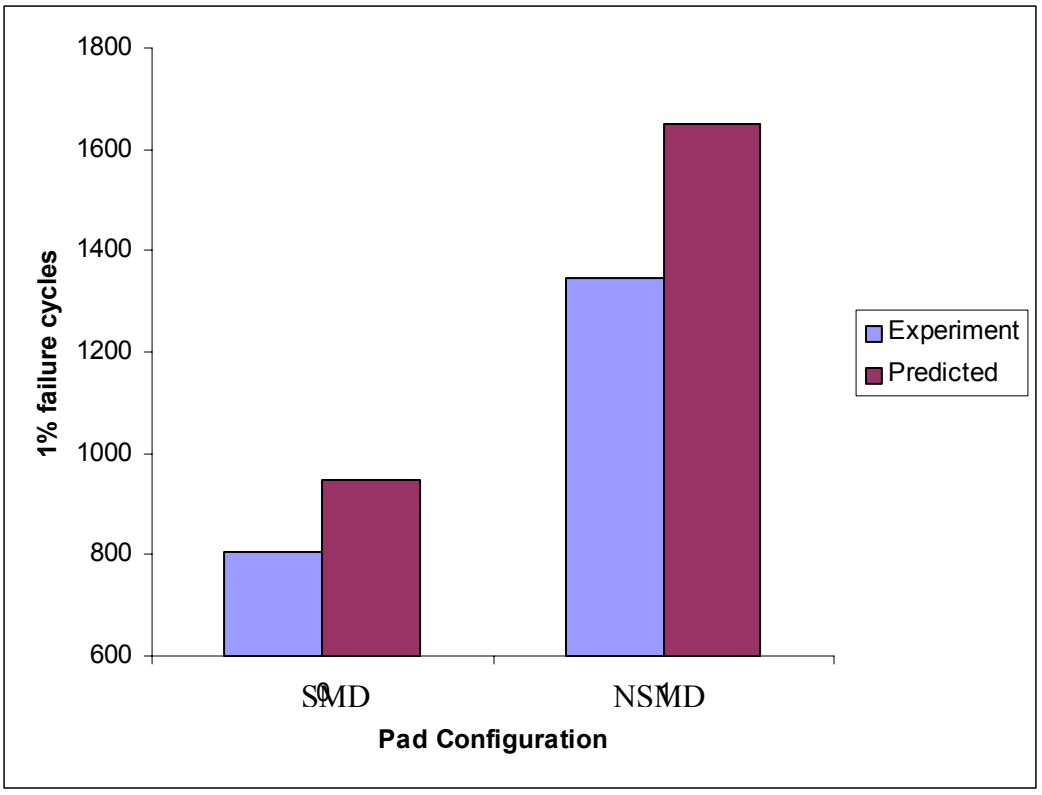

Figure 8 : Effect of change in mask definition from SMD to NSMD on 15mm, 160 I/O FlexBGA thermal reliability.

Device	Experimental X-Factor	Multivariate Regression Model	Sensitivity Factor for Pad Configuration, S_k
15mm, 160 I/O FlexBGA	0.59x	0.57x	0.242

Surface finish:

Experimental data from previous studies indicates that HASL and OSP are significantly more reliable than Electroless Ni/Au for balls grid array packages. This effect has been demonstrated in both rigid-substrate and flex-substrate packages. Packages with compliant elastomeric substrates (e.g. µBGA) may also exhibit this effect.

Hung,S.C. et. al. [2000] investigated the effect of surface finish on the solder joint reliability of 12mm FlexBGA with polyimide substrate, die-up, wire bonded and over-molded configuration. Thermal cycle of –40°C to 125°C with 15mins ramps and 15mins dwells was used for the test. FR-4 test boards of

thickness 0.8mm were used in the test. As seen in fig.9, out of the three surface finishes, the OSP finish boards exhibit maximum thermal reliability. In the plot the value 0 for the board finish corresponds to OSP finish, 1 corresponds to HASL and 2 corresponds to Ni-Au finish. This effect of board finish on the thermal fatigue reliability is attributed to the different inter-metallic system formation for different board finishes. The different inter-metallic systems induce different failure modes thus having impact on the thermal fatigue reliability of the component. Fig.9 demonstrates a close agreement between the experiment and the predicted values from the statistical model.

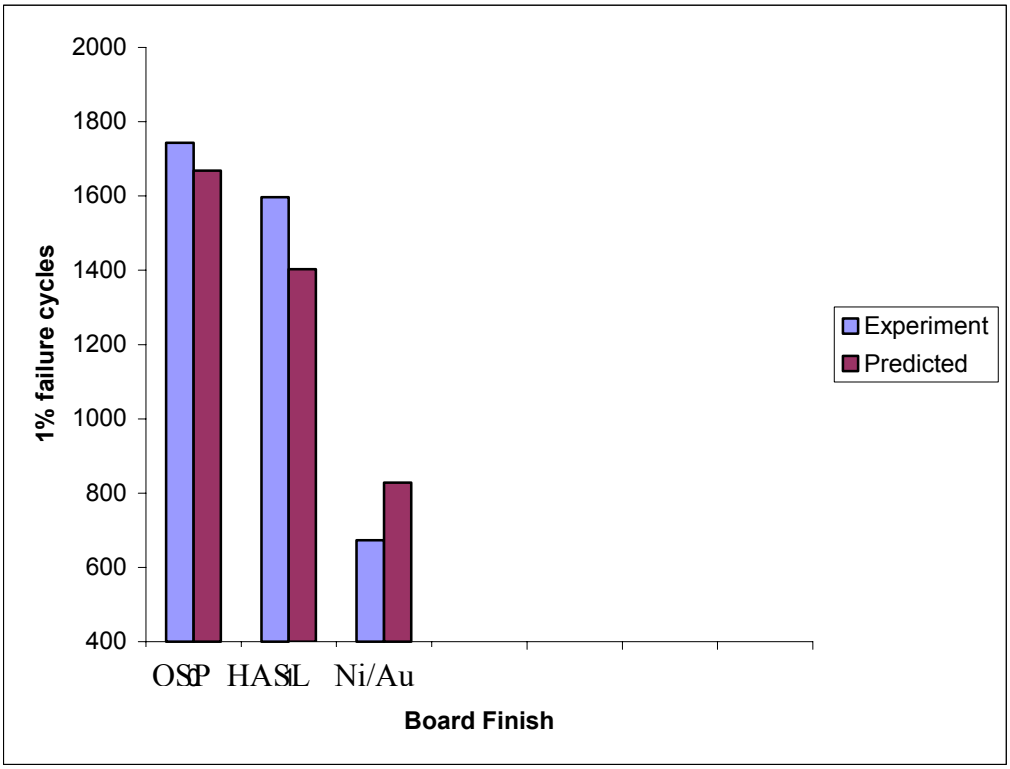

Figure 9: Effect of PCB pad finish on 12mm, 132 I/O FlexBGA thermal reliability subjected to –40 to 125 °C Thermal Cycle

Board Finish	Experimental	Multivariate Regression Model $t_{ref} - S_k\Delta$	Sensitivity Factor for Board Finish, S_k
0 (OSP)	1743	1668	-0.075
1 (HASL)	1597	1403	
2 (Ni-Au)	673	828	

Temperature Cycle Condition:

Temperature cycle condition effects the life of BGA packages under thermal cycling very significantly. The sensitivity of the package thermal reliability to the thermal cycling temperature range has been quantified using the regression analysis in the statistical model. ΔT is the thermal cycling temperature magnitude. The cycles for 1% failure for 12mm, 132I/O FlexBGA with Die/Body ratio of 0.54 predicted by the statistical model has been ploted (Fig.10) with the experimental data from Darveaux et. al. [2000]. Two different temperature cycle conditions used for the comparison are –40°C to 125°C with 15mins of dwell, 15mins ramp and 0°C to 100°C with 30mins of dwell and 30mins of ramp. The experimental data validates the thermal sensitivity of the package predicted by the model.

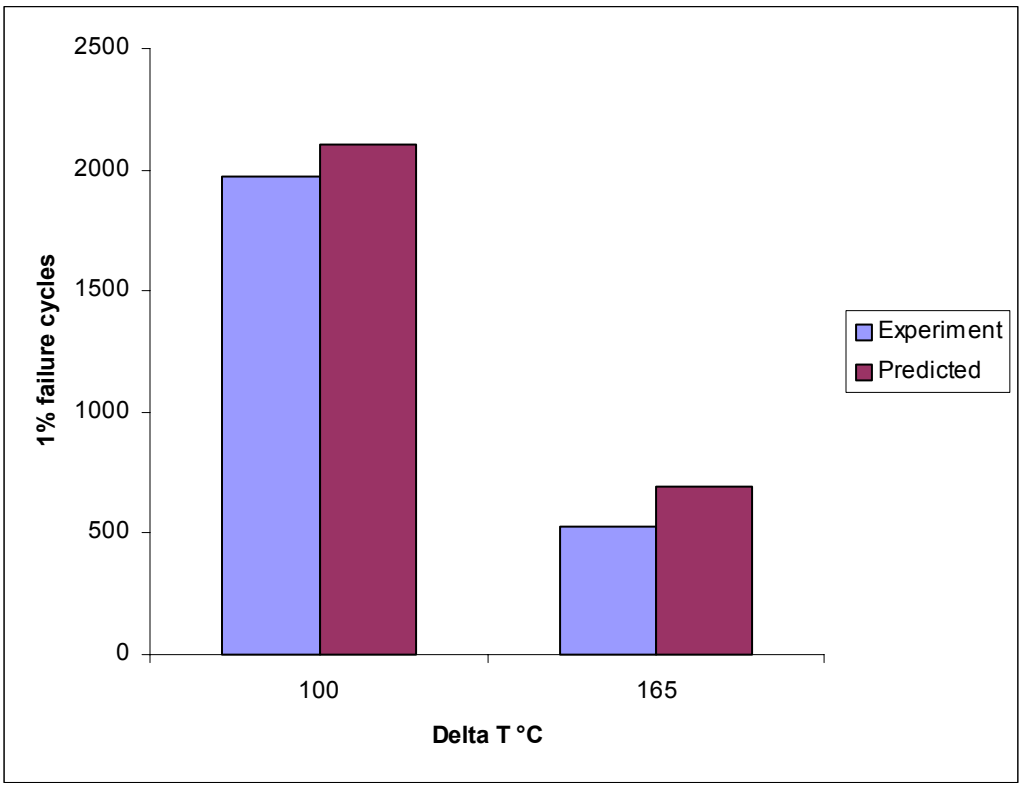

Figure 10: Effect of temperature cycle condition on 12mm, 132 I/O FlexBGA thermal reliability

Device	Experimental X-Factor	Multivariate Regression Model	Sensitivity Factor for PCB Thickness, S_k
12mm, 132I/O FlexBGA	0.27x	0.33x	-0.0037

Statistical Model

Data on FlexBGAs has been statistically analyzed using multivariate regression. Constant and the indices for the following model have been derived. The indices indicate the sensitivity of each of the parameters. The model in its present form is very preliminary and should be used for evaluating relative improvement instead of prediction of absolute value of life. Parameters with "ID" at the end are dummy indices. MasfDefID toggles the mask definition between SMD and NSMD. A value of 0 corresponds to SMD and value of 1 corresponds to NSMD. EMCfilID toggles the mold compound filler content between low and high. A value of 0 corresponds to high filler content and value of 1 corresponds to low filler content. BoardFinishID toggles the board finish between OSP, HASL and Ni-Au finish. 0 corresponds to OSP finish, 1 corresponds to HASL and 2 corresponds to Ni-Au board finish. All the predictor variables except the BoardFinishID are statistically significant with p-values of 0.000. BoardFinishID has p-value of 0.076 which indicates 92.4% confidence level which is little less than the 95.0% confidence level but it has still been included in the model as we know from physics of failure that the board finish has significant effect on the thermal reliability of the BGA packages. A negative value of the index indicates a decrease in time-to-1% failure with increase in value of the variable. Parameters with "MM" at the end indicate that the parameters have been measured in millimeters. Dimensionless parameters including die-to-body ratio and ball count have no units. ΔT is the thermal cycling temperature range measured in °C.

The model finally selected after the regression analysis of all the models is given by the following equation:

$$\mathbf{t_{1\%f} = 3.49(DietoBodyRatio)^{-1.17}(BallCount)^{0.00105}(BallDiaMM)^{1.24}(PCBthkMM)^{-0.193}}$$
$$\mathbf{(EMCFillID)^{0.193}(MaskDefID)^{0.242}(BoardFinishID)^{-0.075}(\Delta T)^{-0.00374}}$$

Table 1: Multivariate Regression Model of FlexBGA Thermal Fatigue Data.

Predictor	Coef	SE Coef	T	P
Constant	3.4935	0.2149	16.26	0.000
DietoBody	-1.1720	0.1133	-10.34	0.000
BallCoun	0.0010451	0.0002191	4.77	0.000
BallDiaMM	1.2438	0.3157	3.94	0.000
PCBthkMM	-0.19297	0.04156	-4.64	0.000
EMCFillID	0.19311	0.04398	4.39	0.000
MasfDefID	0.24159	0.06317	3.82	0.000
BoardFinID	-0.07499	0.04112	-1.82	0.076
DeltaT	-0.0037363	0.0009198	-4.06	0.000

S = 0.09574 R-Sq = 90.0% R-Sq(adj) = 87.9%

Analysis of Variance					
Source	DF	SS	MS	F	P
Regression	8	3.20799	0.40100	43.75	0.000
Residual Error	39	0.35746	0.00917		
Total	47	3.56545			

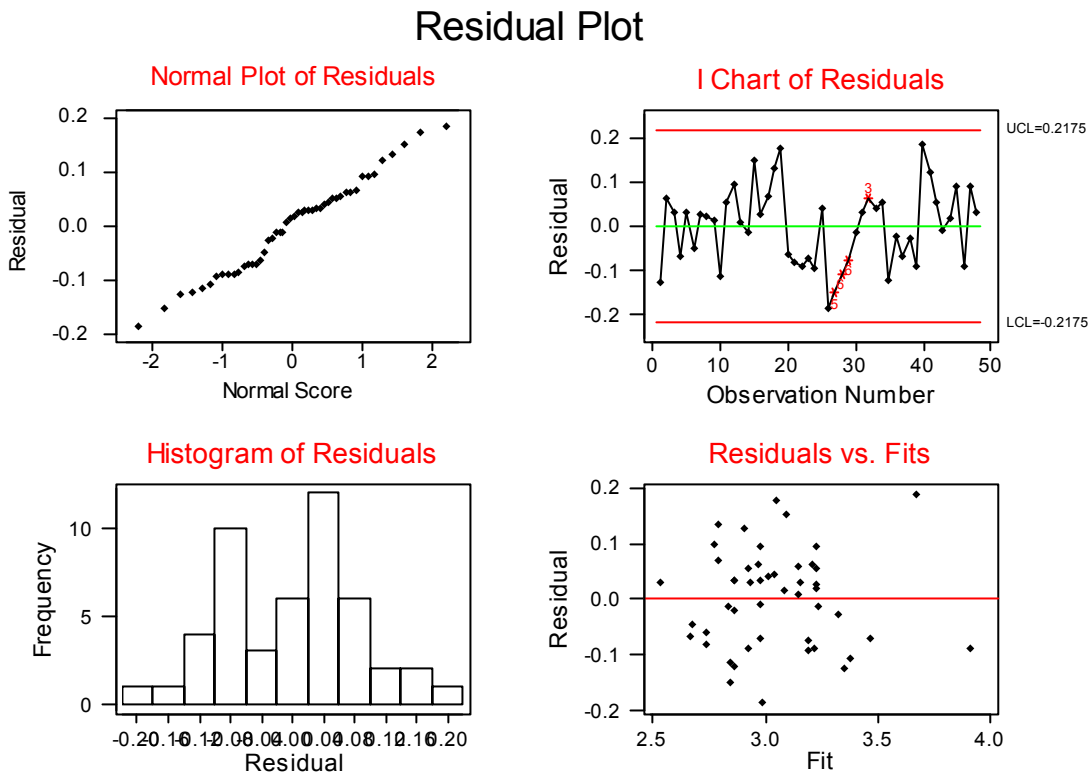

Figure 11: Residual plots for the statistical model

The normal plot of residuals shows approximately a linear pattern closely following a straight line at 45°. Perfectly normal distribution is represented by a straight line at 45° on the normal plot of residuals so the normal plot indicates a fairly normal distribution of the residuals. The histogram plot of residual vs frequency also exhibits a nearly symmetrical bell-shape pattern which is consistent with a sample from a normal distribution. It is important to verify the nature of distribution of the residuals because in the regression analysis for formulating the statistical model we assume the normal distribution of the data. The I-chart of individual observations reveals that the residuals for all the observations are within the three sigma limits of (0.2175, -0.2175) which implies that all the data points in our analysis are fitted within the control limits of 3 sigma. We can see fairly random distribution of the residuals in the residual vs fits plot, which demonstrates the linear relationship between the predictors and the response variable in the model. If

the relationship is not linear than the residuals are distributed following some curved pattern. The plot also holds the assumption of homoskedasticity(constant variance) in the data as the residuals do not fan out or show any pattern as we go from the lower fits to the higher fitted values.

The p-values shown in Table 1 the correspond to a non-zero NULL Hypothesis for coefficient and slope of the regression equation. A low p-value indicates that both the coefficient and slope are statistically significant from zero for the following NULL Hypothesis.

$$H_0 : m = 0 \qquad H_0 : K = 0$$
$$H_A : m \neq 0 \qquad H_A : K \neq 0$$

where m is the coefficient of any variable and K is the intercept on the y-axis, indicated by "constant" in the multivariate regression model.

Other Statistical Models:

Five other statistical models had been tried to fit the thermal reliability data and predict the performance of area array packages under thermal fatigue. This includes linear models, log-linear models and log-log models. The parameter used to check the fitment of the predicted values is cycles to 1% failure. The model finally selected gives the best fit for the predicted values with that of the experimental values. The various models here as under were analyzed.

Linear Regression Model No.1:

Maximum number of predictor variables were used in the basic model to analyze the effect of each variable on the reliability of the package. The various predictors used were BodyMM, DietoBodyRatio, BallCount, BallDiaMM, PitchMM, PCBthkMM, PCBPadDia, EMCFill, MasfDefID, Substrate, BoardFinish, DeltaT and RampRate. Some variables such as EMCFill, MasfDefID, Substrate and BoardFinish did not had numerical values so they were used as dummy variables and each dummy variable was assigned a numerical value. MasfDefID toggles the mask definition between SMD and NSMD. A value of 0 corresponds to SMD and value of 1 corresponds to NSMD. EMCfill toggles the mold compound filler content between low and high. A value of 0 corresponds to low filler content and value of 1 corresponds to high filler content. Substrate toggles the substrate material between polyimide, 2 layer tape laminate and 3 layer tape laminate. A value 0 corresponds to polyamide, value of 1 corresponds to 2 layer tape and value 2 corresponds to 3 layer tape laminate. BoardFinish toggles the board finish between Ni-Au, HASL and OSP. A value of 0 corresponds to Ni-Au, value of 1 corresponds to

HASL and the value of 2 corresponds to OSP finish. The response variable in the regression was the cycles for 1% failure.

The regression equation:

```
1% fail = 3459 +520 BodyMM -3657 DietoBodyRatio -12.3 BallCount
          +7181 BallDiaMM -8629 PitchMM -462 PCBthkMM +3086
          PCBPadDia +264 EMCFill +793 MasfDefID + 15Substrate -230
          BoardFinish -14.3 DeltaT -4.1 RampRate
```

The coefficients in the above equation indicate the sensitivity of each of the parameters. A negative value of coefficient indicates a decrease in time to 1% failure with increase in value of the variable.

Predictor	Coef	SE Coef	T	P
Constant	3459	1663	2.08	0.045
BodyMM	520.2	110.2	4.72	0.000
DietoBod	-3657.1	466.9	-7.83	0.000
BallCoun	-12.342	4.591	-2.69	0.011
BallDiaM	7181	4853	1.48	0.148
PitchMM	-8629	3338	-2.59	0.014
PCBthkMM	-461.6	192.6	-2.40	0.022
PCBPadDi	3086	4795	0.64	0.524
EMCFill	263.9	189.5	1.39	0.173
MasfDefI	792.9	577.6	1.37	0.179
Substrat	14.6	116.1	0.13	0.900
BoardFin	-230.2	188.1	-1.22	0.230
DeltaT	-14.329	5.049	-2.84	0.008
RampRate	-4.08	10.51	-0.39	0.700

S = 392.7 R-Sq = 93.3% R-Sq(adj) = 90.7%

Analysis of Variance

Source	DF	SS	MS	F	P
Regression	13	72832259	5602481	36.33	0.000
Residual Error	34	5243035	154207		
Total	47	78075293			

Correlation coefficient matrix for the predictor variables:

Cell Contents: Pearson correlation

	BodyMM	DietoBod	BallCoun	BallDiaM	PitchMM	PCBthkMM	PCBPadDi	EMCFill
DietoBod	-0.352							
BallCoun	0.924	-0.229						

BallDiaM	0.568	-0.307	0.381					
PitchMM	0.708	-0.368	0.496	0.945				
PCBthkMM	0.221	-0.173	0.101	0.285	0.296			
PCBPadDi	0.580	-0.419	0.303	0.640	0.783	0.391		
EMCFill	-0.018	-0.049	-0.164	0.098	0.097	0.365	0.171	
MasfDefI	-0.342	0.333	-0.201	-0.218	-0.346	-0.280	-0.748	-0.107

	BodyMM	DietoBod	BallCoun	BallDiaM	PitchMM	PCBthkMM	PCBPadDi	EMCFill
Substrat	0.063	-0.001	0.233	-0.107	-0.103	0.175	-0.148	-0.184
BoardFin	-0.063	-0.058	-0.108	0.045	0.036	0.009	0.002	0.100
DeltaT	-0.518	0.441	-0.364	-0.205	-0.314	-0.179	-0.394	-0.125
RampRate	-0.199	0.227	-0.176	-0.040	-0.079	0.091	-0.006	0.017

	MasfDefI	Substrat	BoardFin	DeltaT
Substrat	-0.030			
BoardFin	0.063	-0.420		
DeltaT	0.234	-0.104	0.073	
RampRate	0.109	-0.080	-0.010	0.358

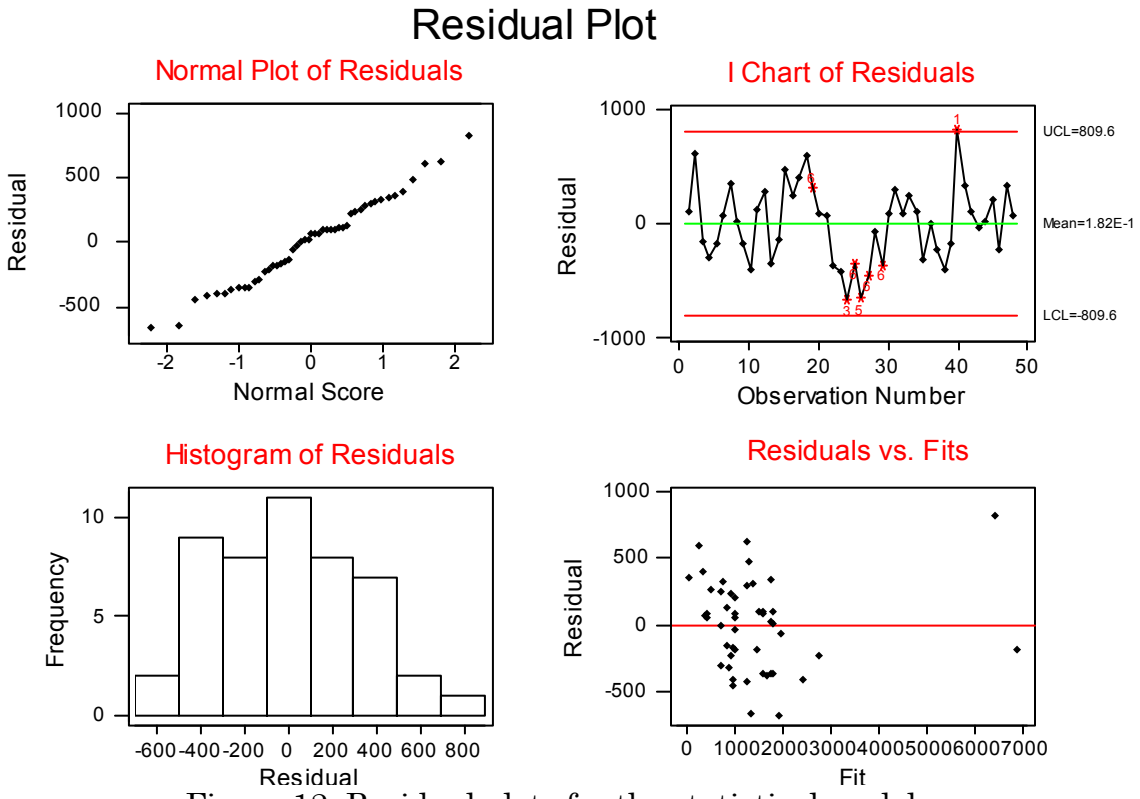

Figure 12: Residual plots for the statistical model

Analyzing the above regression model we see that the model has good R-Sq and R-Sq(adj) value which indicates that more than 90% of variation in the

reliability data is explained by the regression model. But the high p-values of the predictor variables BallDiaM=14.8%, PCBPadDi=52.4%, EMCFill=17.3%, MasfDefI=17.9%, Substrat=90.0%, BoardFin=23.0% and RampRate=70.0% indicate that these variables are statistically insignificant. But from physics of failure we know that these variables have significant effect on the package reliability. Since this statistical insignificance may be attributed to the multi-collinearity among the predictor variables in the reliability data. So we plot the correlation coefficient matrix of the predictor variables and check the correlation coefficients for any multi-collinearity. We see that BallDiaM is highly correlated to PitchMM and has a correlation coefficient of 0.945 where as PCBPadDi is highly correlated to PitchMM and MasfDefI. So we have to neglect both BallDiaM and PCBPadDi from our regression model. We need to run another regression without these two predictor variables and see the effect on the model.

Linear Regression Model No.2:
In this model the same data has been regressed for the formulation of another linear statistical model but the predictors BallDiaM and PCBPadDi have been eliminated due to the multi-collinearity in the previous model.

The regression equation:

```
1% fail = 4617 +506 BodyMM -3674 DietoBodyRatio -12.6 BallCount -
          4149 PitchMM -399 PCBthkMM +250 EMCFill +574 MasfDefID -7
          Substrate -257 BoardFinish -15.0 DeltaT -1.50 RampRate
```

Predictor	Coef	SE Coef	T	P
Constant	4617	1111	4.16	0.000
BodyMM	506.22	94.55	5.35	0.000
DietoBod	-3674.1	468.1	-7.85	0.000
BallCoun	-12.617	3.778	-3.34	0.002
PitchMM	-4149	1008	-4.12	0.000
PCBthkMM	-399.1	187.3	-2.13	0.040
EMCFill	250.2	186.5	1.34	0.188
MasfDefI	573.8	278.4	2.06	0.047
Substrat	-6.9	115.5	-0.06	0.952
BoardFin	-256.6	187.7	-1.37	0.180
DeltaT	-14.994	5.008	-2.99	0.005
RampRate	-1.501	9.322	-0.16	0.873

S = 393.8 R-Sq = 92.9% R-Sq(adj) = 90.7%

Analysis of Variance

Source	DF	SS	MS	F	P
Regression	11	72493777	6590343	42.51	0.000
Residual Error	36	5581517	155042		
Total	47	78075293			

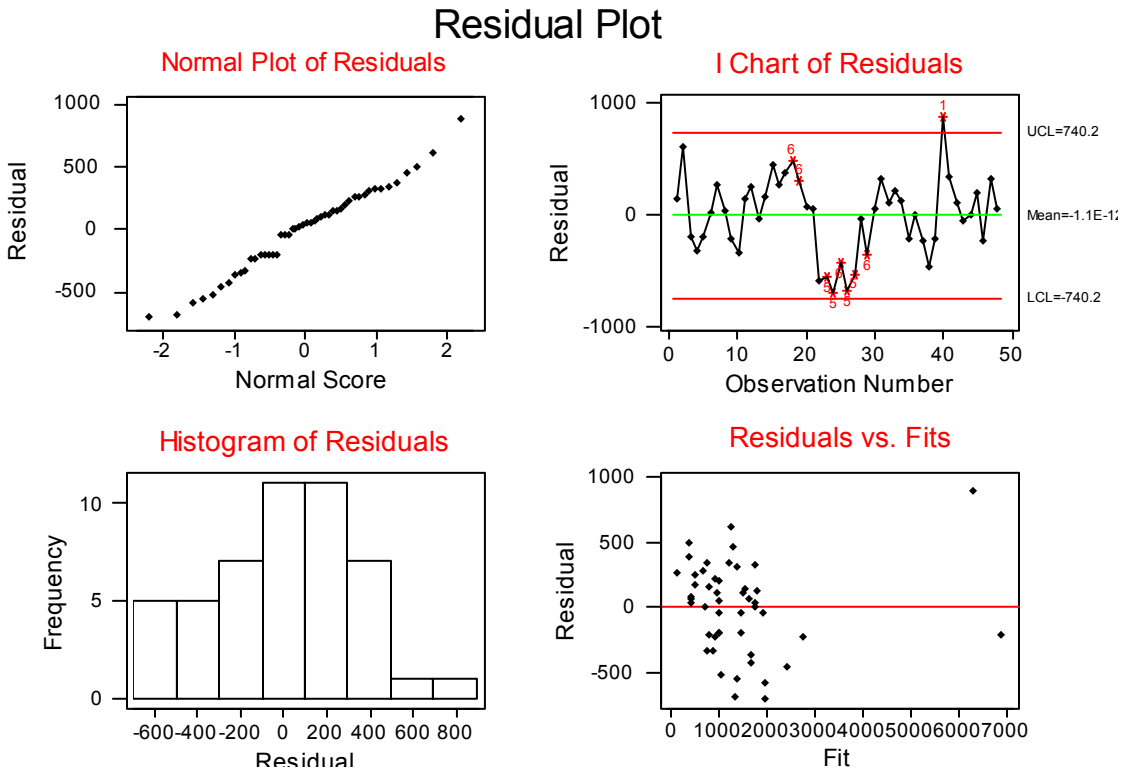

Figure 13: Residual plots for the statistical model

In this model we notice that the R-Sq values remain almost the same so this model also explains more than 90% of the variation in the reliability data. Moreover the p-values for the constant, BallCoun, PitchMM, MasfDefI, BoardFin and DeltaT have improved significantly. But the variables Substrat and RampRate still remain statistically insignificant having very high p-values of 95.2% and 87.3%. The residual-frequency plot indicates non-normality in the distribution of the residuals, which may be because of the statistically insignificant variables. So we would run another regression after eliminating the predictors Substrat and RampRate to see the effect on the model.

Linear Regression Model No.3:

Another linear statistical model has been obtained by regressing the same data, but the statistically insignificant predictors Substrat and RampRate have been dropped from the previous model predictor variables.

The regression equation:

```
1% fail = 4616 +509 BodyMM -3681 DietoBodyRatio -12.7 BallCount -
          4164 PitchMM -408 PCBthkMM +252 EMCFill +573 MasfDefID -
          250 BoardFinish -15.1 DeltaT
```

Predictor	Coef	SE Coef	T	P
Constant	4616.0	941.6	4.90	0.000
BodyMM	508.65	77.49	6.56	0.000
DietoBod	-3680.7	454.0	-8.11	0.000
BallCoun	-12.713	3.002	-4.23	0.000
PitchMM	-4163.7	952.9	-4.37	0.000
PCBthkMM	-407.9	165.8	-2.46	0.019
EMCFill	252.0	180.6	1.40	0.171
MasfDefI	573.2	267.5	2.14	0.039
BoardFin	-250.4	165.6	-1.51	0.139
DeltaT	-15.089	4.415	-3.42	0.002

S = 383.4 R-Sq = 92.8% R-Sq(adj) = 91.2%

Analysis of Variance

Source	DF	SS	MS	F	P
Regression	9	72489404	8054378	54.79	0.000
Residual Error	38	5585890	146997		
Total	47	78075293			

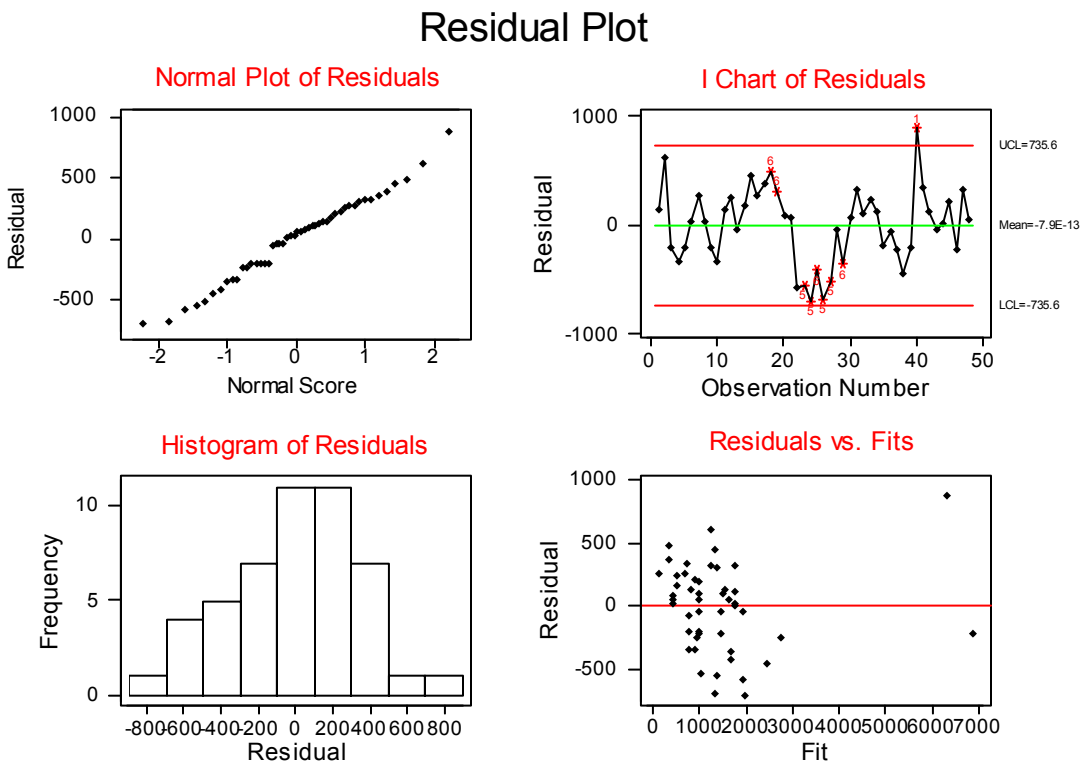

Figure 14: Residual plots for the statistical model

Analyzing the regression results of the model and comparing with the previous model we see that the R-Sq values have increased which shows that this model better explains the variation in the reliability data. There is also improvement in the p-values of the predictor variables BallCoun, PCBthkMM, EMCFill, MasfDefI, BoardFin and DeltaT as compared to the previous model. The p-values for EMCFill(17.1%) and BoardFin(13.9%) are still greater than the significance level of 5%, which means they are statistically insignificant. But we still keep these in our model as from physics of failure we know that they have significant effect on the package reliability. Also these p-values are not too high as in case of the other variables that we dropped from the model.

Log-Linear Regression Model:

In order to see that if the reliability data fits better in a log distribution as compared to the linear distribution we also regressed our reliability data to formulate a log regression model. In this model we initially considered all the predictor variables of the basic linear model but our response variable instead of cycles for 1% failure it is Log of cycles for 1% failure in this case.

The regression equation:

Ln(1%fail) = 3.45 +0.0125 BodyMM -1.17 DietoBodyRatio +0.00057 BallCount +1.45 BallDiaMM -0.163 PitchMM -0.195 PCBthkMM -0.14 PCBPadDia +0.189 EMCFill +0.231 MasfDefID +0.0052 Substrate -0.0730 BoardFinish -0.00339 DeltaT -0.00037 RampRate

Predictor	Coef	SE Coef	T	P
Constant	3.4486	0.4326	7.97	0.000
BodyMM	0.01254	0.02867	0.44	0.665
DietoBod	-1.1711	0.1215	-9.64	0.000
BallCoun	0.000566	0.001194	0.47	0.638
BallDiaM	1.451	1.262	1.15	0.259
PitchMM	-0.1634	0.8682	-0.19	0.852
PCBthkMM	-0.19504	0.05009	-3.89	0.000
PCBPadDi	-0.136	1.247	-0.11	0.914
EMCFill	0.18889	0.04930	3.83	0.001
MasfDefI	0.2315	0.1502	1.54	0.133
Substrat	0.00523	0.03021	0.17	0.864
BoardFin	-0.07296	0.04893	-1.49	0.145
DeltaT	-0.003388	0.001313	-2.58	0.014
RampRate	-0.000374	0.002733	-0.14	0.892

S = 0.1021 R-Sq = 90.1% R-Sq(adj) = 86.2%

```
Analysis of Variance

Source            DF          SS          MS          F          P
Regression        13     3.21073     0.24698      23.67      0.000
Residual Error    34     0.35472     0.01043
Total             47     3.56545
```

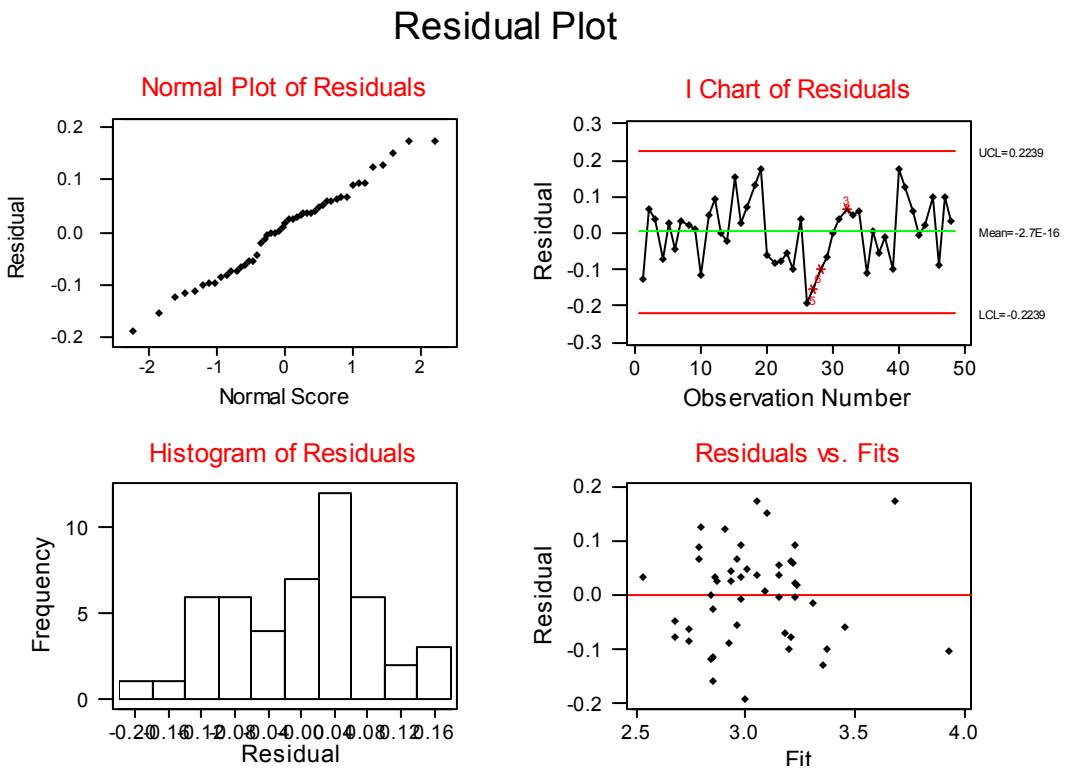

Figure 15: Residual plots for the statistical model

We notice that the R-Sq(adj) value for this model has dropped down below 90%, which means that this model explains only 86.2% of variation in the reliability data. Also the p-values of several predictor variables such as BodyMM, BallCoun, BallDiaM, PitchMM, PCBPadDi, MasfDefI, Substrat, BoardFin and RampRate is more than 10%, which means all these variables are statistically in significant. But we know that this cannot be true. So we can conclude that the log normal distribution does not fit well for this reliability data. If we compare the residual plot for log regression model with the residual plot for the previous model, we can see better normal distribution of the residuals in the previous model.

One reason for this could be that the Log(1% failure cycles) is not directly related to our predictor variables, so we can try to fit different functions of the

predictor variables rather than fitting their values as it is.

Log-Log Regression Model:
In this log regression model we used the log of the predictor variables used in previous model instead of their direct values. This is done to analyze effect of log-log relation between the predictor variables and the response variable on the goodness of fit of the reliability data.

The regression equation:

```
Ln(1%fail)  =  4.44  -1.18LnBodyMM  -1.85LnDietoBodyRatio  +0.944
            LnBallCount  +1.22LnBallDiaMM  +0.44LnPitchMM  -0.513
            LnPCBthkMM    -0.112LnPCBPadDia    -0.0089LnSubstrate
            +0.205LnEMCFill       +0.225LnMasfDefID       -0.0852
            LnBoardFinish -1.12LnDeltaT -0.007LnRampRate
```

Predictor	Coef	SE Coef	T	P
Constant	4.442	1.198	3.71	0.001
LnBodyMM	-1.182	1.138	-1.04	0.306
LnDietoB	-1.8542	0.1967	-9.42	0.000
LnBallCo	0.9443	0.5169	1.83	0.076
LnBallDi	1.220	1.399	0.87	0.389
LnPitchM	0.436	1.689	0.26	0.798
LnPCBthk	-0.5135	0.1319	-3.89	0.000
LnPCBPad	-0.1115	0.7851	-0.14	0.888
LnSubstr	-0.00888	0.02951	-0.30	0.765
LnEMCFil	0.20479	0.04784	4.28	0.000
LnMasfDe	0.2248	0.1171	1.92	0.063
LnBoardF	-0.08516	0.04860	-1.75	0.089
LnDeltaT	-1.1199	0.5479	-2.04	0.049
LnRampRa	-0.0073	0.1606	-0.05	0.964

```
S = 0.09923     R-Sq = 90.6%     R-Sq(adj) = 87.0%

Analysis of Variance

Source            DF          SS          MS          F         P
Regression        13     3.23068     0.24851     25.24     0.000
Residual Error    34     0.33478     0.00985
Total             47     3.56545
```

Correlation coefficient matrix for the different variables:

```
Cell Contents: Pearson correlation

       LnBodyMM LnDietoB LnBallCo
LnDietoB -0.271
```

LnBallCo	0.914	-0.025						
LnBallDi	0.649	-0.298	0.380					
	LnBodyMM	LnDietoB	LnBallCo	LnBallDi	LnPitchM	LnPCBthk	LnPCBPad	LnSubstr
LnPitchM	0.748	-0.345	0.477	0.968				
LnPCBthk	0.203	-0.196	0.082	0.259	0.267			
LnPCBPad	0.580	-0.428	0.293	0.692	0.790	0.382		
LnSubstr	0.076	0.017	0.220	-0.100	-0.097	0.188	-0.160	
LnEMCFil	-0.037	-0.066	-0.170	0.090	0.087	0.359	0.172	-0.184
LnMasfDe	-0.295	0.349	-0.165	-0.193	-0.290	-0.280	-0.683	-0.030
LnBoardF	-0.038	-0.034	-0.070	0.053	0.049	0.004	0.022	-0.420
LnDeltaT	-0.414	0.487	-0.268	-0.185	-0.269	-0.180	-0.380	-0.104
LnRampRa	-0.346	0.446	-0.240	-0.132	-0.200	-0.057	-0.226	-0.112

	LnEMCFil	LnMasfDe	LnBoardF	LnDeltaT
LnMasfDe	-0.107			
LnBoardF	0.100	0.063		
LnDeltaT	-0.125	0.234	0.073	
LnRampRa	-0.067	0.209	0.039	0.831

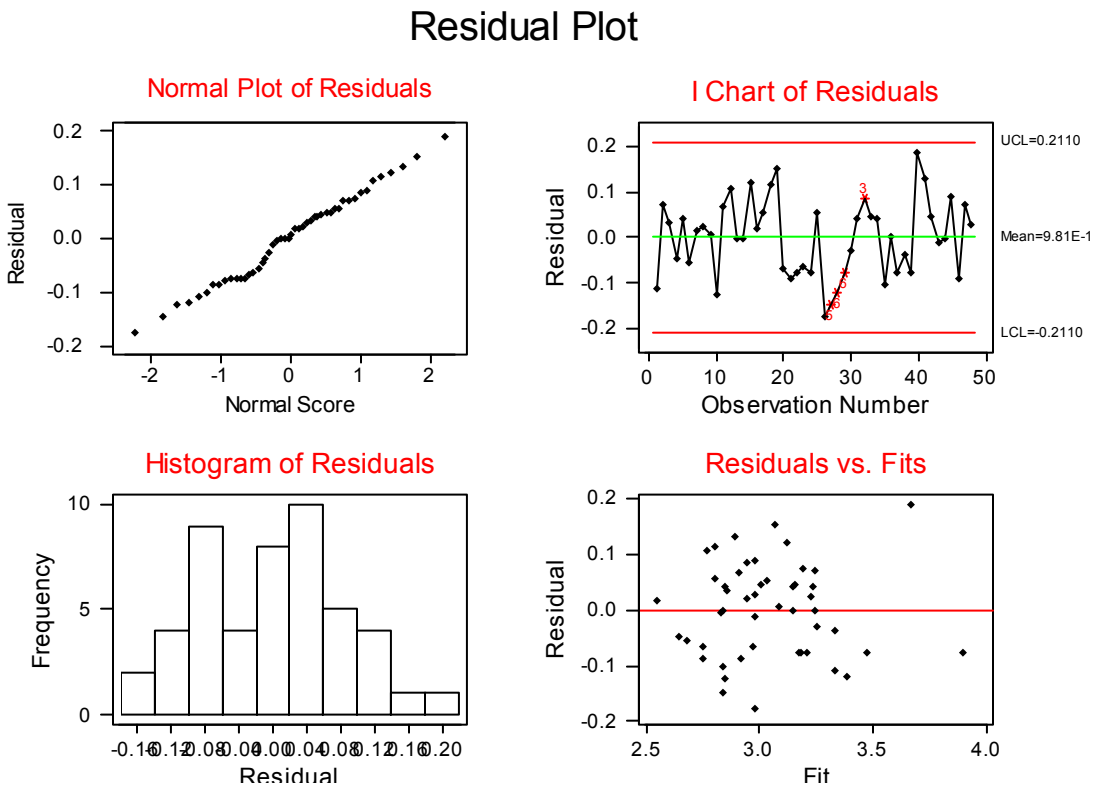

Figure 16: Residual plots for the statistical model

We observe that the residual distribution is still not fairly normal but better than our previous model. R-Sq(adj) is still much less than 90.0% only 87.0% of the variation in the reliability data is explained by this model. Also the p-values of most of the predictors is quite high: LnBodyMM=30.6%, LnBallDi=38.9%, LnPitchM=79.8%, LnPCBPad=88.8%, LnSubstr=76.5% and LnRampRa=96.4%. There is also multi-collinearity among the various predictor variables. This indicates that log-log relation does not hold between the predictors and the response variable.

Closed-form Model Library

In the simplest terms - a closed form model is a model of the form

$$y = \sum_{i=0}^{n} c_i f(x_i) \qquad (1)$$

which has a unique & non-trivial solution that can be obtained in a non-iterative manner. Reliability prediction involves material properties, geometry and architecture, pad stacks, assembly stiffness, global mismatch, local mismatch, crack initiation and propagation relationships and damage superposition (Figure 17). Typically, this class of problems has been addressed using non-linear finite-element models which incorporate the non-linear constitutive behavior of solder and other non-linear materials in the structure. This tool DOES NOT involve using finite-element models. In order to incorporate and address product reliability upfront in the design process - CLOSED-FORM models have been developed based on the non-linear FE models to pro-actively provide first-order reliability estimates of the product reliability up-front in the design phase.

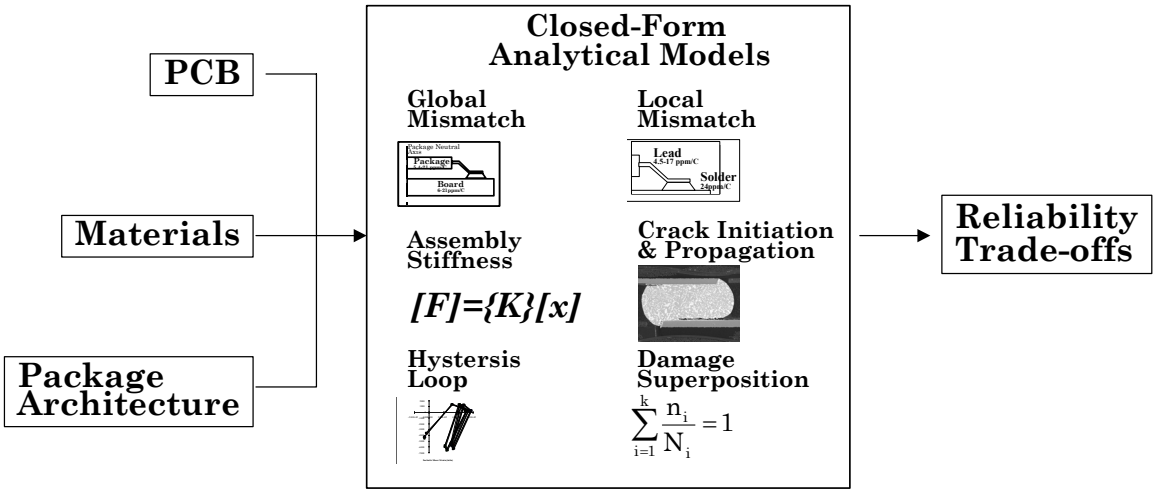

Figure 17: Inputs and outputs from the Closed-form Model Library.

This section describes the approach used in the development of closed-form model library. The model library in its present form addresses thermal fatigue in the strain rate regime of 10^{-3} to 10^{-4} in/in/sec. While thermal fatigue modeling is discussed in this paper - readers interested in understanding other failure mechanisms should refer to [Lall, et. al. 1997].

Elastic-plastic behavior

The total strain in the solder joints can be identified into three regimes (a). Elastic (b). Plastic (c). Creep. Hall [1991] showed that for fast temperature ramps there was little creep relaxation during the temperature ramp - after arriving at the new temperature, the sample creeps or stress relaxes till the temperature is changed again. Based on this, during loading & unloading the time independent stress-strain curve (i.e. the elastic + plastic portion) is assumed to be purely elastic with a slope of G_{eff} (Figure 18). This approach has also been used by several other researchers including - Clech, Knecht and Fox . In the loading regime, the form of constitutive law taken is of the form.

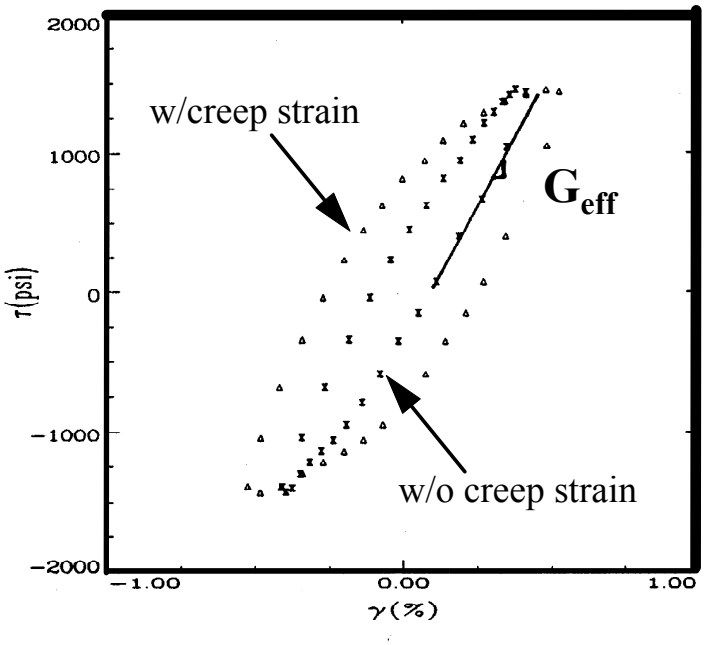

Figure 18: Hystersis loop for solder during temperature cycling - with and without creep strain [Knecht and Fox 1991].

$$\gamma_{total} = \gamma_{elastic} + \gamma_{plastic} + \gamma_{creep}$$

$$\gamma_{elastic+plastic} = \frac{\tau}{G_{eff}} + \left(\frac{\tau}{\tau_p}\right)^2 \qquad (2)$$

where G_{eff} is the slope of linear unloading regime, τ_p is the plasticity parameter, τ is the shear stress, γ is the shear strain.

Table 2: Value of the Plasticity Parameter as a function of Temperature [Knecht and Fox 1991].

Values of Plasticity Parameter	
Temperature (°C)	τ_p (psi)
25°C	41900
60°C	34700
100°C	19500

Creep relationship

Constitutive behavior of the solder has been modeled using a Sinh-Viscoplastic law [Brown et.al. 1989]

$$d^p = Ae^{-\frac{Q}{RT}} Sinh\left(\xi \frac{\sigma}{s}\right)^{\frac{1}{m}} \quad (3)$$

where, the dynamic hardening is represented by

$$\frac{ds}{dt} = \left(h_0 \left|1 - \frac{s}{s^*}\right|^a sign\left(1 - \frac{s}{s^*}\right)\right) d^p \quad (4)$$

and,

$$s^* = \tilde{s}\left(\frac{d^p}{A} e^{\frac{Q}{RT}}\right) \quad (5)$$

where, d^p is the effective inelastic deformation resistance, σ is the effective cauchy stress, s is the deformation resistance, s^* is the saturation value of the deformation resistance, $\tilde{s}$ is the coefficient of deformation resistance saturation value, A is the pre-exponential, Q is the activation energy, m is the strain rate sensitivity, h_0 is the constant rate of thermal hardening, and T is absolute temperature. The deformation resistance represents the isotropic resistance to inelastic flow of the material. The material parameters in this constitutive equation, A, Q, m, ξ, h_0, $\tilde{s}$, and a are assumed to be temperature independent in the temperature and strain range of interest.

Lumped Parameter Approach

A lumped parameter approach has been used to describe the substrate or component versus PC board interaction during thermal cycling in terms of solder joint shear and assembly stiffness (Figure 19). The lumped parameter formulation is based on the fact that the thermal mismatch is accommodated in the shear of the solder and the bimetallic strip bending of the assembly.

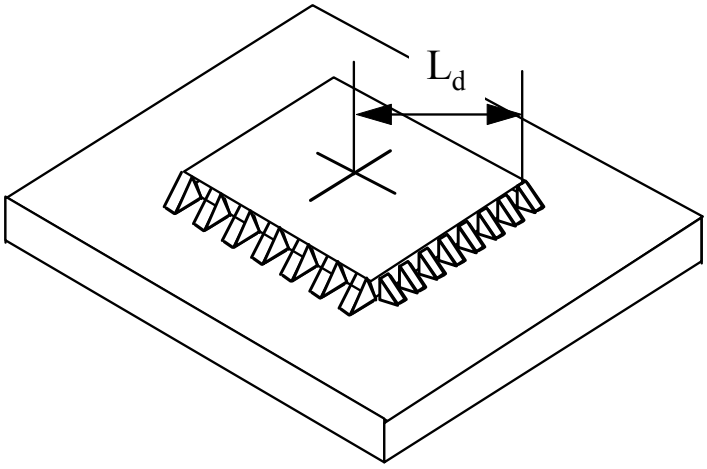

Figure 19: Lumped Parameter Approach.

$$\gamma + \frac{\tau}{\kappa} = \gamma_{th\_max}$$

$$\gamma_{th\_max} = \frac{L_d}{h}\left|\alpha_{pwb} - \alpha_{prt}\right|\left(T - T_o\right) \qquad (6)$$

$$\kappa = \frac{K_a h}{a}$$

where γ is the total shear strain, τ is the nominal shear stress, κ is the characteristic stiffness of assembly (which is a function of global and local stiffness), L_d is the diagonal distance to farthest solder joint, h is the solder joint height, a is the solder joint area, T_o is the reference temperature, T is the Temperature, α_i = CTE of i; i =PWB & Part respectively.

Global Stiffness

The equivalent stiffness of the assembly is determined by a combination of three spring stiffness (a). tensile component stiffness (K_1) (b). tensile board stiffness (K_2) (c). bending stiffness of assembly (K_3).

$$\frac{1}{K} = \frac{1}{K_1} + \frac{1}{K_2} + \frac{1}{K_3}$$

$$\frac{E_p^t h_p}{\left(1-\nu_p\right)} = \sum_{i=1}^{N} \frac{E_i^t h_i}{\left(1-\nu_i\right)} \qquad (7)$$

$$\frac{E_p^t h_p^3}{12\left(1-\nu_p\right)} = \sum_{i=1}^{N} \frac{E_i^t h_i^3}{12\left(1-\nu_i\right)}$$

The effective properties for tensile and flexural modulus has been used to evaluating the global stiffness relation. The mathematical relationships for K_1,

K_2, K_3 have been developed based on models available in literature & bi-metallic beam theory.

Local Stiffness

The local stiffness is based on the Kotlowitz [1991] lead equations for gull-wing and J-leads which relate the lead geometry to the structural stiffness in the x, y and z directions.

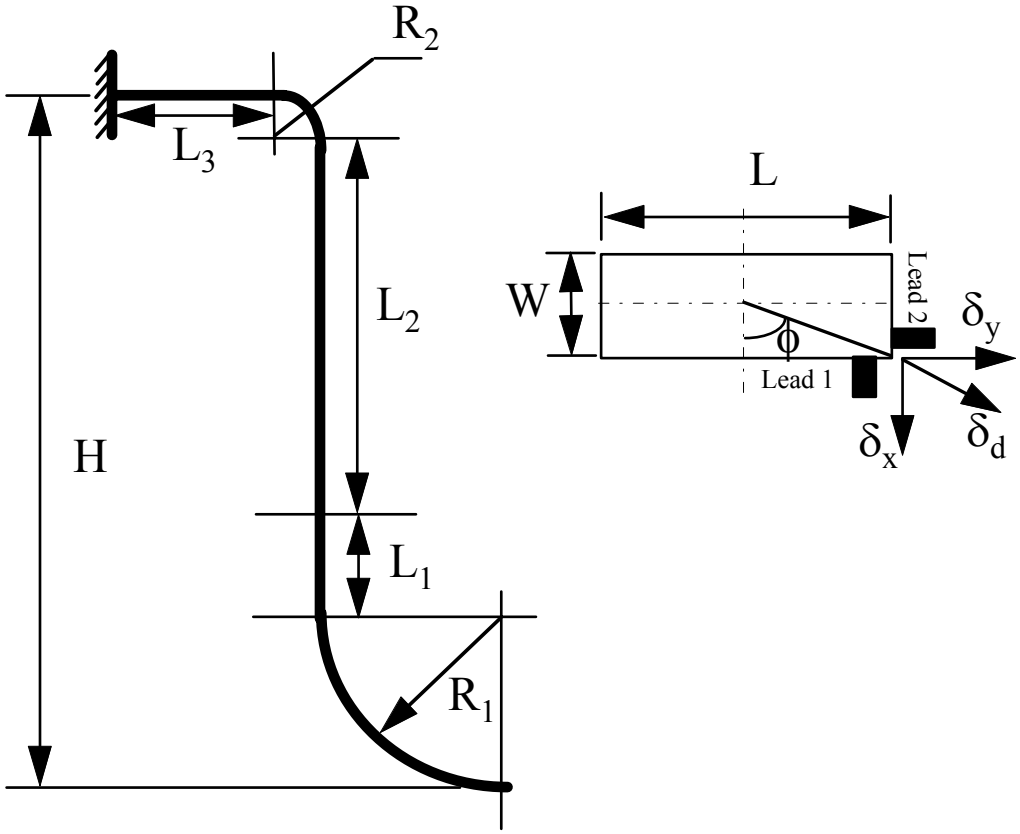

Figure 20: Kotlowitz parametrization of the lead geometry [Kotlowitz 1991].

$$K_{d,2} = \frac{K_x K_y \sqrt{1+r^2}}{\sqrt{K_x^{\,2} + r^2 K_y^{\,2}}}$$

$$K_{d,1} = \frac{K_x K_y \sqrt{1+r^2}}{\sqrt{r^2 K_x^{\,2} + K_y^{\,2}}} \qquad (8)$$

where K_x and K_y are the stiffnesses along the x and y axes respectively, r is the ratio of the package length to the width, and K_d is the diagonal stiffness. The subscripts 1 and 2 represent the diagonal stiffness for lead on edges 1 and 2 on the package (Figure 20).

References

Brown, S.B., Kim, K.H., Anand, L., "An Internal Variable Constitutive Model for Hot Working of Metals", International Journal of Plasticity, Vol.5, pp.95-130, 1989

Darveaux,R., Heckman,J., Sayed,A., and Mawer,A., "Solder Joint Fatigue Life of Fine Pitch BGAs-Impact of Design and Material Choices", Microelectronics Relaibility, Volume 40, Issue 7, pp. 1117-1127, July2000.

Darveaux, R. and Mawer, A., "Solder joint fatigue life of fleXBGA assemblies", Electronic Components and Technology Conference, 1998. 48th IEEE, pp. 707-712, 25-28 May 1998.

Ghaffarian,R., "Technology Readiness Overview: Ball Grid Array and Chip Scale Packaging", http://nepp.nasa.gov NEPP Program Document, January 2003.

Ghaffarian, R. and Kim, N.P., "Reliability and failure analyses of thermally cycled ball grid array assemblies", Electronic Components and Technology Conference, 1998. 48th IEEE, pp. 713-720, 25-28 May 1998.

Hall, P.M.,"Forces, moment, and displacements during thermal chamber cycling of leadless ceramic chip carriers soldered to printed boards", IEEE Transactions on CPMT, 1984, Vol. 7, No. 4, December 1994, pp.314-327

Hall, P.M., "Creep and Stress Relaxation in Solder Joints", Solder Joint Reliability edited by John Lau, Van Nostrand and Reinhold, New York, 1991

Hall, P.M.,"Creep and Stress Relaxation in Solder Joints in Surface-Mounted Chip carriers," Proceedings of Electronic Components Conference (ECTC), Boston, MA,1987, May 11-13, pp.579-588.

Hung,S.C., Zheng,P.J., Lee,S.C., Ho,S.H., and Chen,H.N., "Thermal Cyclic Fatigue of the Interconnect of a Flex-Type BGA", Proceedings of 50th Electronic Component and Technology Conference, pp. 1384-1391, Las Vegas, Nevada, May21-24,2000.

Kotlowitz, R. W.,"Comparative Compliance of Representative Lead Designs for Surface Mounted Components", Proceedings of the IEEE Electronic Components Conference (ECTC), Houston, TX, May 22-24, 1989, pp.791-831.

Knecht, S., and Fox, L.,"Integrated Matrix Creep: Application to Accelerated Testing and Lifetime Prediction"; Chapter 16, *Solder Joint Reliability: Theory*

and Applications, edited by John Lau, Van Nostrand Reinhold, 1991, pp. 508-544.

Lall, P., Pecht, M., Hakim, E., "Influence of Temperature on Microelectronic and System Reliability", CRC Press, Boca Raton, Florida 1997.

Levis, K.M.and Mawer, A., "Assembly and solder joint reliability of plastic ball grid array with lead-free versus lead-tin interconnect", Electronic Components and Technology Conference, 2000. 50th Proceedings, pp. 1198-1204 Las Vegas, Nevada, May21-24, 2000.

Mawer, A., Cho, D., and Darveaux, R., "The effect of PBGA solder pad geometry on solder joint reliability", Poc. SMI, 1996, pp. 127-135.

Mawer,A, "Motorola Semiconductor Technical Data-Plastic Ball Grid Array", AN1231, pp. 1-28, November 1996.

Mawer, A., Vo, N., Johnson, Z. and Lindsay, W., "Board-level characterization of 1.0 and 1.27 mm pitch PBGA for automotive under-hood applications", Electronic Components and Technology Conference, Proceedings 49th, pp. 118-124, 1999.

Mercado, L.L., Sarihan, V., Guo, Y. and Mawer, A, " Impact of solder pad size on solder joint reliability in flip chip PBGA packages**",** Advanced Packaging, IEEE Transactions, Volume: 23 Issue: 3, pp. 415-420, Aug 2000.

Muncy, J., Lazarakis, T. and Baldwin, D, "Predictive Failure Model of Flip Chip on Board Component Level Assemblies", Electronic Components and Technology Confrence, pp. 578-582, 2003.

Thompson, T.; Carrasco, A.; Mawer, A., "Reliability assessment of a thin (flex) BGA using a polyimide tape substrate", Electronics Manufacturing Technology Symposium, Twenty-Fourth IEEE/CPMT, pp. 207-213, 1999.

Whiteman, L., "Electronic Miniaturization for Missile Applications" EMMA Program, American Competitiveness Institute. http://tag.empf.org

Appendix-I

Table 2(data set 1-5)

Package	PBGA		flexBGA		flexBGA		flexBGA		flexBGA		
Body(mm)	15	17	7.5	7.5	8	8	8	8	8	8	8
Die(mm)	6.5x6.5	8.7x8.7	3.5x3.5	3.5x3.5	3.5x3.5	3.5x3.5	6.5x6.5	6.5x6.5	3.5x3.5	5.2x5.2	6.5x6.5
Die/Body	0.43	0.51	0.47	0.47	0.44	0.44	0.81	0.81	0.44	0.65	0.81
Ball Count	160	256	40	40	96	96	96	96	96	96	96
Ball Dia(mils)	20	20	18	18	12	12	12	12	12	12	12
Pitch(mm)	1.0	1.0	0.8	0.8	0.5	0.5	0.5	0.5	0.5	0.5	0.5
PCB thk(mm)	1.6	1.6	0.85	1.6	0.85	1.6	0.85	1.6	0.85	0.85	0.85
mask/pad(mm)	.55/.40	.55/.40	.45/.30	.45/.30	.40/.25	.40/.25	.40/.25	.40/.25	.40/.25	.40/.25	.40/.25
Substrate	Lam	Lam	2LTape	2LTape	2LTape	2LTape	2LTape	2LTape	2LTape	2LTape	2LTape
EMC filler	low	low	low	low	low	low	low	low	low	low	low
PCB mat CTE	4-layer FR4 (2S2P) CTE-17.1ppm/°										
Ball Material											
Solder Paste											
1st fail	2006	1358	1781	1990	3209	2600	454	410	3209	846	454
Mean life	2525	2000	2082	2403	NA	NA	555	582	NA	1050	555
Variable	Die/Body, Ball count		PCB thk		PCB thk		PCB thk		Die/Body		

Table 3 (data set 6-10)

Package	flexBGA		flexBGA		flexBGA		flexBGA		flexBGA	
Body(mm)	8	8	8	8	12	12	12	12	12	12
Die(mm)	5.2x5.2	5.2x5.2	5.2x5.2	5.2x5.2	6.4x6.4	6.4x6.4	9.5x9.5	9.5x9.5	6.4x6.4	9.5x9.5
Die/Body	0.65	0.65	0.65	0.65	0.53	0.53	0.79	0.79	0.53	0.79
Ball Count	96	96	96	96	132	132	132	132	132	132
Ball Dia(mils)	12	12	12	12	18	18	18	18	20	20
Pitch(mm)	0.5	0.5	0.5	0.5	0.8	0.8	0.8	0.8	0.8	0.8
PCB thk(mm)	0.85	0.85	0.85	0.85	0.85	1.6	0.85	1.6	1.6	1.6
mask/pad(mm)	.40/.25	.40/.25	.40/.25	.40/.25	.43/.33	.43/.33	.43/.33	.43/.33	.43/.33	.43/.33
Substrate	3LTape	3LTape	3LTape	2LTape	3LTape	3LTape	3LTape	3LTape	2LTape	2LTape
EMC filler	low	high	low	low	low	low	low	low	low	low
PCB mat CTE	4-layer FR4 (2S2P) CTE-17.1ppm/°									
Ball Material										
Solder Paste										
1st fail	898	507	898	846	2201	1574	1053	858	1748	741
Mean life	1319	986	1319	1050	3922	2998	1426	1265	3123	984
Variable	EMC filler		Substrate		PCB thk		PCB thk		Die/Body	

Table 4 (data set 11-15)

Package	flexBGA		flexBGA		flexBGA		flexBGA		flexBGA	
Body(mm)	12	12	12	12	12	12	12	12	12	12
Die(mm)	9.5x9.5	9.5x9.5	9.5x9.5	9.5x9.5	9.5x9.5	6.4x6.4	6.4x6.4	6.4x6.4	6.4x6.4	9.5x9.5
Die/Body	0.79	0.79	0.79	0.79	0.79	0.53	0.53	0.53	0.53	0.79
Ball Count	144	144	144	144	144	144	132	132	144	144
Ball Dia(mils)	18	18	18	18	18	18	18	18	18	18
Pitch(mm)	0.8	0.8	0.8	0.8	0.8	0.8	0.8	0.8	0.8	0.8
PCB thk(mm)	0.85	1.6	1.6	1.6	0.85	0.85	1.6	1.6	1.6	1.6
mask/pad(mm)	.43/.33	.43/.33	.43/.33	.43/.30	.43/.33	.43/.33	.43/.33	.33/.43SMD	.43/.33	.43/.33
Substrate	3LTape	3LTape	3LTape	3LTape	2LTape	2LTape	3LTape	3LTape	3LTape	3LTape
EMC filler	low	low	low	low	high	high	low	low	low	low
PCB mat CTE	4-layer FR4 (2S2P) CTE-17.1ppm/°									
Ball Material										
Solder Paste										
1st fail	1055	844	844	980	527	1794	1574	642	2020	844
Mean life	1563	1308	1308	1528	698	2230	2998	1082	2967	1308
Variable	PCB thk		mask/pad		Die/Body		mask/pad		Die/Body	

Table 5 (data set 16-20)

Package	flexBGA		flexBGA		flexBGA		flexBGA		flexBGA	
Body(mm)	15	15	15	15	15	15	16	16	16	16
Die(mm)	7.3x7.3	7.3x7.3	9.5x9.5	9.5x9.5	12x12	12x12	8.5x8.5	8.5x8.5	8.5x8.5	8.5x8.5
Die/Body	0.49	0.49	0.63	0.63	0.80	0.80	0.53	0.53	0.53	0.53
Ball Count	160	160	208	208	208	208	280	280	280	280
Ball Dia(mils)	20	20	18	18	18	18	18	18	18	18
Pitch(mm)	1.0	1.0	0.8	0.8	0.8	0.8	0.8	0.8	0.8	0.8
PCB thk(mm)	1.6	1.6	0.85	1.6	0.85	1.6	0.85	0.85	0.85	1.6
mask/pad(mm)	.58/.43	.43/.53SMD	.45/.30	.45/.30	.45/.30	.45/.30	.45/.30	.45/.30	.45/.30	.45/.30
Substrate	2LTape	2LTape	2LTape	2LTape	2LTape	2LTape	3LTape	3LTape	3LTape	3LTape
EMC filler	low	low	low	low	low	low	low	high	low	low
PCB mat CTE	4-layer FR4 (2S2P) CTE-17.1ppm/°									
Ball Material										
Solder Paste										
1st fail	1500	920	1538	1454	693	542	2081	1519	2081	1907
Mean life	2005	1316	2738	2352	875	708	2802	2348	2802	2740
Variable	mask/pad		PCB thk		PCB thk		EMC filler		PCB thk	

Table 6 (data set 21-24)

Package	flexBGA		flexBGA		flexBGA		MAP	
Body(mm)	16	16	16	16	16	16	15	15
Die(mm)	11.5x11.5	11.5x11.5	11.5x11.5	11.5x11.5	11.5x11.5	8x8	6.8x6.8	10.5x10.2
Die/Body	0.72	0.72	0.72	0.72	0.72	0.50	0.45	0.69
Ball Count	280	280	280	280	280	280	196	196
Ball Dia(mils)	18	18	18	18	18	18	16	20
Pitch(mm)	0.8	0.8	0.8	0.8	0.8	0.8	1.0	1.0
PCB thk(mm)	0.85	0.85	0.85	1.6	0.85	0.85	1.6	1.6
mask/pad(mm)	.45/.30	.45/.30	.45/.30	.45/.30	.45/.30	.45/.30	.38/.50	.38/.50
Substrate	3LTape	3LTape	3LTape	3LTape	3LTape	3LTape	Lam	Lam
EMC filler	low	high	low	low	high	high	NA	NA
PCB mat CTE	4-layer FR4 (2S2P) CTE-17.1ppm/°							
Ball Material								
Solder Paste								
1st fail	1500	920	1538	1454	693	542	2081	1519
Mean life	2005	1316	2738	2352	875	708	2802	2348
Variable	mask/pad		PCB thk		PCB thk		EMC filler	

Table 7 (data set 25-26)

Package	flexBGA			flexBGA		
Body(mm)	12	12	12	12	12	12
Die(mm)	9.0x9.0	9.0x9.0	9.0x9.0	6.5x6.5	6.5x6.5	6.5x6.5
Die/Body	0.75	0.75	0.75	0.54	0.54	0.54
Ball Count	132	132	132	132	132	132
Ball Dia(mils)	0.45	0.45	0.45	0.45	0.45	0.45
Pitch(mm)	0.8	0.8	0.8	0.8	0.8	0.8
PCB thk(mm)	0.8	0.8	0.8	0.8	0.8	1.6
mask/pad(mm)	SMD	SMD	SMD	SMD/NSMD	SMD/NSMD	SMD/NSMD
Substrate	polyimide	polyimide	polyimide	polyimide	polyimide	polyimide
EMC filler	NA	NA	NA	NA	NA	NA
PCB mat CTE	FR-4					
Ball Material						
Solder Paste						
1st fail	1567	1749	No failure	2647	2844	1180
Mean life						
Variable	HASL	OSP	HASL with encp.	HASL	OSP	Ni/Au

Table 8 (data set 27-29)

Package	flexBGA		flexBGA		flexBGA	
Body(mm)	15	15	12	12	12	12
Die(mm)	7.3x7.3	7.3x7.3	6.4x6.4	6.4x6.4	9.5x9.5	9.5x9.5
Die/Body	0.49	0.49	0.53	0.53	0.79	0.79
Ball Count	160	160	132	132	144	144
Ball Dia(mils)	20	20	18	18	18	18
Pitch(mm)	1.0	1.0	0.8	0.8	0.8	0.8
PCB thk(mm)	1.6	1.6	1.6	1.6	1.6	1.6
mask/pad(mm)	.58/.43	.43/.53SMD	.43/.33	.33/.43SMD	.43/.33	.43/.30
Substrate	2LTape	2LTape	3LTape	3LTape	3LTape	3LTape
EMC filler	low	low	low	low	low	low
PCB mat CTE	FR-4					
Ball Material						
Solder Paste						
1st fail	1500	920	1574	642	844	980
Mean life	2005	1316	2998	1082	1308	1528
Variable	mask/pad		mask/pad		mask/pad	

Table 9 (data set 30-31)

Package	PBGA	PBGA	PBGA	PBGA
Body(mm)	23	23	23	23
Die(mm)	10x10	10x10	10x10	10x10
Die/Body	0.43	0.43	0.43	0.43
Ball Count	324	324	324	324
Ball Dia(mils)	0.6	0.6	0.6	0.6
Pitch(mm)	1.0	1.0	1.0	1.0
PCB thk(mm)	0.79	0.79	0.79	0.79
mask/pad(mm)	.5/.51SMD	.5/.51SMD	.5/.51SMD	.5/.51SMD
Substrate	NA	NA	NA	NA
EMC filler	NA	NA	NA	NA
PCB mat CTE	FR-4			
Ball Material	62Sn36Pb2Ag	62Sn36Pb2Ag	96.5Sn3.5Ag	96.5Sn3.5Ag
Solder Paste	63Sn37Pb	95.5Sn3.8Ag0.7Cu	63Sn37Pb	95.5Sn3.8Ag0.7Cu
1st fail				
Mean life	2583	2126	3573	no failure
Variable				

Table 10 (data set 32-33)

Package	PBGA	PBGA	PBGA	PBGA
Body(mm)	23	23	23	23
Die(mm)	10x10	10x10	10x10	10x10
Die/Body	0.43	0.43	0.43	0.43
Ball Count	324	324	324	324
Ball Dia(mils)	0.6	0.6	0.6	0.6
Pitch(mm)	1.0	1.0	1.0	1.0
PCB thk(mm)	0.79	0.79	0.79	0.79
mask/pad(mm)	.5/.51SMD	.5/.51SMD	.5/.51SMD	.5/.51SMD
Substrate	NA	NA	NA	NA
EMC filler	NA	NA	NA	NA
PCB mat CTE	FR-4			
Ball Material	62Sn36Pb2Ag	62Sn36Pb2Ag	96.5Sn3.5Ag	96.5Sn3.5Ag
Solder Paste	63Sn37Pb	95.5Sn3.8Ag0.7Cu	63Sn37Pb	95.5Sn3.8Ag0.7Cu
1st fail				
Mean life	4555	4520	6019	no failure
Variable				